

Spatial and temporal variations of upper mesospheric winds inferred by using successive images of noctilucent clouds observed in Iceland.

Ryoma Yamashita¹, *Hidehiko Suzuki¹

1. Department of physics, Meiji university

Injection of momentum through dissipations of gravity waves propagated from lower atmosphere and active productions of minor constituents caused by precipitation of energetic particles are known as dominant sources of disturbances in upper mesosphere. Since some of these disturbances occur locally and intermittently, it is important to know time constant (i.e. diffusivity) against such impulsive fluctuations on momentum and concentration of minor constituents to understand the energy and mass budgets in the upper mesosphere. One of the straight methods to know the amplitude of the eddy diffusion is to measure the spatial distribution of wind field with high temporal resolution. In this study, derivation of spatial and temporal variation of upper mesospheric winds by tracking a motion of noctilucent cloud (NLC) observed by a ground-based color digital camera in Iceland is conducted. The procedure for wind field estimation consists with 3 steps; (1) projects raw images to a geographical map (2) enhances NLC structures by using FFT method (3) determines horizontal velocity vectors by applying template matching method to two sequential images. In this talk, a result of the wind derivation by using successive images of NLC with 3 minutes interval and ~1.5h duration observed on the night of Aug 1st, 2013 will be reported as a case study.

Keywords: Noctilucent cloud, wind field, mesopause, upper mesosphere

Development of the electron density automatic estimation algorithm in the ionosphere lower region

*Taketoshi Miyake¹, Ryota Nakazawa¹, Yuki Ashihara²

1. Department of Informatic system, Faculty of Engineering, Toyama Prefectural University, 2. National Institute of Technology, Nara College

In the lower ionosphere, the approximate electron density profile can be estimated from the comparison between these observation results obtained by sounding rocket and propagation characteristics calculated with Full wave method. This estimation process, which is so-called " wave absorption method" , has some problems. At first, we have no clear standard for comparing observation results and propagation characteristics calculated with Full wave method. In addition, we have to iterate many times correcting the electron density profile by handwork, calculating propagation characteristics with Full wave method and comparing observation results and calculated propagation characteristics. This iteration takes too long to estimate appropriate electron density profile. To reduce these problems, we developed an application to realize automated estimation of electron density profile by analyzing radio wave propagation characteristics.

In the previous study, they succeeded to estimate accurate electron density profile in the ionosphere automatically in very short time. In the estimated electron density profile, however, there was an unnatural sudden fluctuation of the electron density in low-altitude region. We improved the estimation algorithm and succeeded to estimate natural electron density profile automatically.

Keywords: ionospheric lower region, Full-wave method, altitude profile of electron density

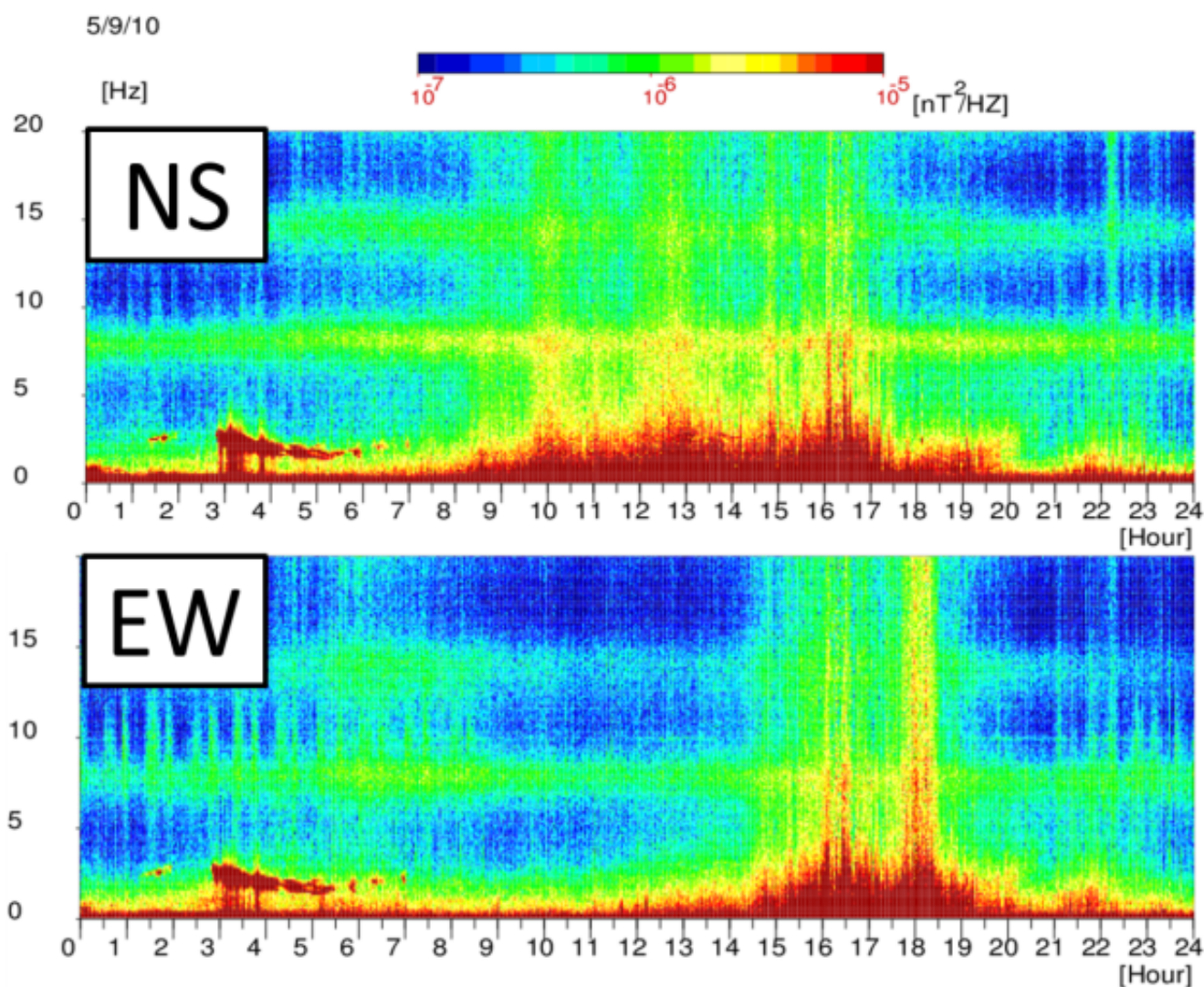
Difference between North-South and East-West components of ELF magnetic disturbances associated with lightning detected at Kawatabi, Osaki, Miyagi, Japan

*Tomoko Nakagawa¹, Syota Takahashi¹, Kotaro Nishiyama¹

1. Information and Communication Engineering, Tohoku Institute of Technology

In the record of 0.1-20 Hz Extremely Low Frequency (ELF) magnetic variations observed by using two sets of induction magnetometers for NS and EW components, there found cases where broadband disturbances were present only in one of the two components. Intense disturbance was found in EW component in 6 out of 8 events found at Kawatabi, in the absence of NS disturbances. It would suggest the orientation of the source lightning near the observation site.

Keywords: ELF, lightning, magnetic variation, East-West, induction magnetometer, direction



Low cost applications in astronomy, atmospheric science and communications using radio waves forward scattering from meteor trails

*Waleed Madkour¹, Masa-yuki Yamamoto¹

1. Kochi University of Technology

The forward scattering of VHF radio signals by meteor ionized trails incorporates unique characteristics for usage in various applications. The oblique incidence of radio signals off the meteor trails enables the detection of fainter meteors using low-power transmitters. The relatively long duration of the scattered signals reflects the meteor trails behavior in relation to the atmospheric conditions near the meteor altitude region. It can also be used in communication of short bursts of data between distant locations on earth. In this research work, the usage of the forward scattering of radio waves by the meteor ionized trails in astronomy, upper atmospheric science and communication is presented. The developed meteor observation system follows the classical forward scattering setup commonly used worldwide. A methodology using locally developed software applications and interferometry technique to track the direction of each meteor echo is described as a fundamental step towards trajectory observations and hence meteor origins determination. Through using the same setup and software, the role of the secondary mesospheric ozone layer in oxidizing the meteor ionized trails was examined through meteor echoes duration distribution analysis during two meteor showers; the Perseids and the Geminids. Preliminary observations of the indirect link between solar cycle sun spot activity level and the meteor echo duration analysis is also presented. The observational research approach relies on extending the capabilities of the amateur basic setups by software automation in an attempt to fill the wide gap between the amateur systems and the professional ones. The gap that is mainly due to the difference in the amount of observational data each system can provide, can be partially filled through automation to provide enough data for statistical analysis. The methodology along with sample observational results for each application is described in detail as a proof of concept. The sample observational results in astronomy and upper atmospheric science applications are generally in agreement with the fundamentals of meteor science. Nevertheless, more statistical results are still required for further verification. In line with the observational activities, a practical meteor burst communication (MBC) study was performed to explore the feasibility of using modern technologies such as D-STAR ham-radio network and Android to simplify the MBC system. Although no positive results were obtained, the concept needs to be examined by higher power transmitters to compensate for the higher frequency used in the 144 MHz range. The three presented applications are not isolated from each other and the overlaps between them are highlighted. The low cost system setups introduced can be a model for low budget institutes planning to build a practical setup for educational as well as scientific purposes. The developed software applications are made free for use worldwide in order to support similar research themes.

Keywords: Meteor ionized trails, Radio Forward scatter, Interferometry

The development of software defined FMCW ionosonde based on the GNU Radio (2)

*Hiromitsu Ishibashi¹, Takuya Tsugawa¹, Takumi Kondo¹, Mamoru Ishii¹

1. National Institute of Information and Communications Technology

We are developing a GNU Radio based software defined FMCW ionosonde system.

The initial result has been already presented at the SGPSS 2016 fall meeting: as for the receiving system, we successfully got ionograms using the transmitting system of current FMCW ionosonde in Kokubuji and the

Ettus Research USRP N210. One of the main purposes of this work is to inherit peripheral units of current FMCW ionosonde system, which is currently operated in the Southeast Asia low-latitude ionospheric network (SEALION).

So, we have adopted X300 USRP instead of N210 and updated programs which is suitable for X300.

The additional frontend unit necessary to inherit peripheral units of current FMCW ionosonde system is being manufactured now.

This presentation is a subsequent follow-up report for these past 6 months.

Expansion of ionospheric TEC observation from measurements of single frequency GPS signals

*Yoshitaka Goto¹, Win Zaw Hein¹, Atsushi Matsui¹, Yoshiya Kasahara¹

1. Graduate School of Natural Science and Technology

Monitoring of the ionospheric total electron content (TEC) using observational networks of GNSS signals is now popular in many countries. Most of the networks are built in mid latitude regions. It is important to expand them in low latitudes where many interesting phenomena of ionospheric plasma exist. The purpose of this study is to develop an estimation method of the ionospheric TEC using not multi-frequency receiver but single frequency ones, and expand an observation network in low latitude region at low costs.

Two observables are obtained from single frequency GPS measurements; code pseudorange and carrier phase. In these observables, the ionospheric effect appears plus and minus, respectively. The ionospheric effect is, then, derived by their difference while it includes a bias error. For the estimation of the bias error, the TEC distribution is assumed to be represented by two-dimensional (latitude-longitude) model with a polynomial function in each dimension. A thin layer model is assumed for altitude distribution of the ionospheric plasma. Ranging errors except for the ionospheric effect and receiver clock error in code pseudorange measurements are removed using precise ephemeris and existing appropriate models. Accuracy of the bias estimation is a few TECU that is equivalent to standard deviation of measurement error of the code pseudorange.

We are now planning to build continuous observation site in a low latitude region.

Keywords: Single frequency GPS signal, Ionospheric TEC, Bias estimation

N_2^+ resonant scattering light observation in the sunlit topside ionosphere with the auroral spectrograph

*Yu Endo¹, Takeshi Sakanoi¹, Yasunobu Ogawa², Masato Kagitani¹

1. Planetary Plasma and Atmospheric Research Center, Graduate School of Science, Tohoku University, 2. National Institute of Polar Research

We report the ground-based optical remote-sensing of molecular ion upflow by measuring 427.8 nm N_2^+ resonant scattering in the sunlit topside ionosphere. *Störmer* [1955] has summarized his work on sunlit aurora from 1918 to 1943. He observed the sunlit aurora extending to 700-1100 km altitude and the strong emission from N_2^+ . *Bates* [1949] suggested the N_2^+ emission at 427.8 nm is resonant scattering in the sunlit region. Recently, satellite data showed N_2^+ emission at the high altitude in the range from 400 to about 1,000 km. MSX satellite observed first the N_2^+ emission probably caused by N_2^+ upflow from the topside ionosphere [*Romick et al.*, 1999]. Ion upflow is essential for the source of ion outflow observed in the magnetosphere. O^+ ion upflow happens mainly during geomagnetically disturbed conditions [*Moen et al.*, 2004, *Abe et al.*, 1993]. Furthermore, the heavier molecular ions which mainly exist in the E-region were also measured at about 10,000 km altitudes [*Yau et al.*, 1993]. However, the mechanism of these molecular ion upflow is uncertain. Now, we think that N_2^+ created by the charge exchange between N_2 and O^+ in F-region are upflowing during geomagnetically disturbed condition. Thus, we focus on N_2^+ 427.8 nm emission caused not by auroral precipitating electrons but by resonant scattering in the sunlit topside ionosphere associated with N_2^+ upflow using the data taken by Aurora Spectrograph (ASG) at Longyearbyen, Svalbard (geographic latitude : 75.2 deg and geographic longitude : 16:04 deg) for 13 years.

The ASG consists of a fish-eye lens, slit, grism and a cooled CCD detector which covers the wavelength range of 420-730 nm with a 2.0 nm spectral resolution and field of view of 180° along the magnetic meridian. The ASG have been operating since 2000, but measuring N_2^+ emission 427.8 nm since 2004. The preceding study figured out that there is a high probability that the N_2^+ outflow occurs in geomagnetically disturbed condition ($Kp > 4$) [*Mizuno et al.*, 2005]. Therefore, we analyzed the 65 events during from 2004 to 2016 which the sun does not illuminate the ground and the Kp indices were greater than 4 for more than 9 hours. Then, if a single aurora arc appears in the geomagnetically southward direction, we can regard the auroral distribution as the auroral height profile. In this case, we can roughly assume the emission height with the simultaneous 557.7 and 630.0 nm emission. The oxygen emission at 557.7 nm is considered to be caused only by precipitating electrons, and if the 427.8 nm emission is distributed higher (larger elevation angle) than 557.7 nm, this 427.8 nm emission is resonant scattering light. We found 5 events in this cases of all 65 events. The Kp indices of these events are 4-, 2+, 3+, 4-, 6-, 5, and we found that there were two cases which are during geomagnetically disturbed conditions and not disturbed ones. Around 0700 UT on December 21, 2014 ($Kp=2+$), the maximum 427.8 nm emission is 400 R and Dst indice is -10 nT (an hour before the 427.8 nm observation). Then, the 427.8 nm emission peak is assumed to be at 380 km if the 630.0 nm emission peak is considered to be at 250 km. While, around 0100 UT on December 21, 2015, a geomagnetic storm occurred (Dst indice is -150 nT), and N_2^+ emission was observed at intensity of 800 R. Then, N_2^+ emission peak is 340 km and the emission at intensity more than 200 R extended up to 1,000 km and more. Of all 5 events, the N_2^+ emission peak is in 300~400 km in 4 events, the altitudes which the intensity are less than 200 R are higher increasing the activity of geomagnetism. This result suggests that N_2^+ is produced in the lower F-region and then upflowing with the geomagnetic activity. This is consistent with the preceding study.

Keywords: aurora, nitrogen molecular ion, up flow

Estimation of global scale airglow structure by observation from International Space Station

*Yusuke Kitamura¹, Akinori Saito¹, Takeshi Sakanoi², Yuichi Otsuka³, Atsushi Yamazaki⁴, Yuta Hozumi¹

1. Department of Geophysics, Graduate School of Science, Kyoto University, 2. Planetary Plasma and Atmospheric Research Center, Graduate School of Science, Tohoku University, 3. Institute for Space-Earth Environmental Research, Nagoya University, 4. Institute of Space and Astronautical Science / Japan Aerospace Exploration Agency

We analyzed the dependence of large scale structure of night time airglow at 630 nm on the local time, latitude and longitude using ISS-IMAP/VISI observation data from the International Space Station and analyzed the IRI model TEC, IRI and MSIS airglow model .

ISS-IMAP/VISI is an airglow observer installed in the International Space Station for about 3 years from September 2012 to August 2015. It observes 630 nm airglow. At 630 nm, the airglow is emitting at around 250 km altitude, and the emission due to the equatorial anomaly has a dominant influence. We examined the dependence of 630nm airglow on local time, latitude and longitude, and compared it with the previous study. In the equator, it seemed that the latitude of the north and south became maximum at around 15 degrees due to equator anomaly. The equatorial anomaly weakened from the night to the morning and disappears, but it was observed that the observation was brightening around midnight and things like midnight temperature maximum were confirmed. Also, the asymmetry between the north and south hemisphere of the seasonal variation was confirmed. Similar asymmetry was observed in the 40 degrees north and south where the influence of equatorial anomaly was small.

In addition, we compared and verified the results of these results, total electron number data by IRI model which is an ionosphere model, and emission intensity of 630 nm airglow calculated from IRI model and MSIS model which is the atmosphere model.

Relationship between electron density height profile and convection flow speed in the polar cap patches and blobs

*Fukizawa Mizuki¹, Takeshi Sakanoi¹, Yasunobu Ogawa², Yoshimasa Tanaka², Keisuke Hosokawa³, Satoshi Taguchi⁴, Evan Thomas⁵

1. Planetary Plasma and Atmospheric Research Center, Graduate School of Science, Tohoku University, 2. National Institute of Polar Research, 3. Department of Communication Engineering and Informatics, University of Electro-Communications, 4. Department of Geophysics, Graduate School of Science, Kyoto University, 5. Dartmouth College

We focus on the enhanced electron density in the ionospheric F region associated with polar patches and blobs using the data taken with European Incoherent Scatter (EISCAT) radar and all-sky imager at Longyearbyen. Polar patches are regions of high-density plasma in the polar cap F-region. They are thought to be generated by expansion of the polar cap convection driven by pulsed reconnection [Lockwood and Carlson, 1992] and transported anti-sunward by $\mathbf{E} \times \mathbf{B}$ drift. Subsequently they exit polar cap and evolve into blobs in the sunward return flow region of closed field line. These phenomena play important role on electron density fluctuations in the polar cap and high-latitude ionosphere. However detailed processes controlling the electron density distribution are not understood well. EISCAT Svalbard Radar (ESR) observed the enhanced electron density in the F-region associated with polar patches 1730 to 2230 UT (2000-0100 MLT) on 11 January 2016. We interpreted that it is not caused by auroral electron precipitation because there is no enhanced electron density in the E-region and no enhanced ion temperature in the F-region. The direction of IMF was southward during 1530-1640 UT, 1730-1820 UT and 1930-2350 UT. Compared with the simultaneous OI (630.0 nm) emission all-sky images, eleven polar patches were identified. We find that the electron density profiles in the polar patches were classified into the two groups as follows: One is that electron density was enhanced in the altitude range from 300 to 500 km. The other is that the enhancement in electron density ranged from 250 to 350 km altitudes. On the other hand, SuperDARN data showed that the ion velocity in the polar cap in the latter case were higher than that in the former case. Thus, we suggest that this difference would be caused by the difference of ion convection speed in the polar cap as described in the following mechanism. When the ion velocity is high, the difference between the ion and neutral velocity becomes large and then the ion temperature increases by frictional heating. The increased ion temperature contributes to the growth of rate coefficients of $\text{O}^+ + \text{N}_2 \rightarrow \text{NO}^+ + \text{O}$ and $\text{O}^+ + \text{O}_2 \rightarrow \text{O}_2^+ + \text{O}$ reactions [Schunk et al., 1976]. Consequently, electron density decreases by $\text{NO}^+ + e \rightarrow \text{N} + \text{O}$ and $\text{O}_2^+ + e \rightarrow \text{O} + \text{O}$ reactions. At high altitudes, NO^+ and O_2^+ density due to the enhanced NO^+ and O_2^+ scale heights with the increased ion temperature. Additionally, the successive electron density enhancements in the F region were observed by EISCAT Tromsø UHF Radar from 2037 to 2100 UT (2200 to 2230 MLT) on the same day. Simultaneous GPS-TEC map data indicates that it was probably caused by blobs in the closed field region originated from the polar cap. This interval was in the recovery phase of substorm according to AE index. Since the polar cap boundary shrinks in the substorm recovery phase, we suggest that Tromsø located into the sunward return flow region in the dusk convection cell, and then blobs passed over Tromsø.

Keywords: polar patch, blob

Statistical estimation of growth time of medium-scale traveling ionospheric disturbances by three dimensional spectral method

*Takafumi Ikeda¹, Akinori Saito¹

1. Department of Geophysics, Graduate School of Science, Kyoto University

Medium scale traveling ionospheric disturbance is one of phenomenon in ionosphere and has been long studied. Nighttime MSTID will be caused by Perkins instability. Linear growth time(e folding time) of Perkins instability is very slow as growth time from random thermal noise . Therefore , we expect explanation of growth of MSTID by including electric field of Sporadic E layer . However, we have not almost estimated observational growth time of MSTID.

Using this method, we statistically estimated growth rates of nighttime MSTID in japan in summer 2014 observed by GNSS. We used 3DFFT for total electron content(TEC) grid data ,and estimated propagation velocity. Using this velocity, we tracked movement of one wavefront of MSTID. We estimated the maximum growth time of each event by using wavenumber spectra when tracking. As a result, growth time is slower than 16 minutes. Propagation direction when growth time is fastest is southwestward(205° - 245°). Growth time is maximum when 240°. This magnitude is too slow as growth time of MSTID, and is within the range of one perkins instability expects. We will show the detail about the relation between this growth time and both mechanisms, and also show the solar activation and the seasonal dependence of growth time.

Keywords: Medium-scale traveling ionospheric disturbances, GPS-TEC, Perkins instability, Three dimensional spectral method

Role of gravity waves in the upper atmospheric temperature changes in association with sudden stratospheric warming

*Changsup Lee¹, In-Sun Song¹, Hwajin Choi¹, Jeong-Han Kim¹, Geonhwa Jee¹

1. Korea Polar Research Institute

Fourier Transform Spectrometers (FTSs) at the Esrange space center (67°53'N, 21°04'E), Kiruna, Sweden and at the Dasan Korean Arctic station (78°55'N, 11°56'E), Svalbard, Norway have observed mesospheric air temperature from OH airglow emissions near 87 km height since November 2002. The FTS observations have provided simultaneous mesospheric temperature at the two different latitudes in association with elevated stratopause (ES) after major stratospheric sudden warming (SSW) events. ES-like phenomena and relevant warming have been simulated using global circulation models such as the whole-atmosphere community climate model (WACCM), but the model prediction is found to be much weaker mesospheric warming compared with the FTS and satellite observations especially in polar region such as the Dasan station. Considering that gravity waves (GWs) may have substantial impacts on the temperature and wind in the upper atmosphere, the discrepancy between observation and model may be attributed to common issues in GW parameterizations: Uncertainty in GW spectra and unrealism in GW propagation (i.e., columnar propagation). In this study, we investigate effects of the horizontal propagation and refraction of GWs on mesospheric warming associated with the ES after major SSW events using a ray-tracing model with specified GW spectra. Preliminary results for steady background flows show that the horizontal propagation and refraction increase westward GW momentum forcing near $z = 100$ km in the NH high latitudes that can induce downward motions and adiabatic warming in the NH polar regions below $z = 100$ km. Results are extended for time-varying background flows and different GW spectra to consider tidal effects and improve robustness of results, respectively.

Keywords: sudden stratospheric warming, gravity wave, ray tracing

Spatial Distributions of Total Electron Content Variations Associated with Earthquakes

Shun Shomura¹, *Hiroyuki Nakata¹, Hiroyo Ohya¹, Toshiaki Takano¹, Takuya Tsugawa², Michi Nishioka²

1. Graduate School of Engineering, Chiba University, 2. National Institute of Information and Communications Technology

The coseismic ionospheric disturbances are generated by the acoustic wave and atmospheric gravity wave excited by earthquakes. In the previous studies, it is found that the perturbations of total electron content (TEC) are correlated with the magnitude of the earthquake. On the other hand, the relationship between the magnitude and the spatial distributions of these perturbations are not examined in detail. Using two-dimensional TEC maps derived from the GNSS Earth Observation Network (GEONET), in this study, we have analyzed the spatial distributions of TEC variations associated with earthquakes. First of all, the TEC distribution map is divided in grid whose size is 0.2 x 0.2 degrees. The spectral intensity of the TEC perturbations is calculated using Fast Fourier Transform. The average of the spectral intensity in each grid is determined from those in the ionospheric pierce points (altitude = 350 km) located with in each grids. After the center of the TEC variation distributions are determined from the average map, the latitudinal and longitudinal width of the TEC perturbations are estimated by fitting the perturbations with the Gaussian function. We analyzed 5 earthquakes ($M > 6.8$) whose epicenters are located at the sea around Japan since 2000. The wave recorders installed by the Japan Meteorological Agency observed the heights of tsunamis. Using these data, the heights of tsunamis in the epicenter are determined using Green's theorem, which explains the relationship between the height of tsunami and the depth of the sea. The results of the fitting shows that the latitudinal width of TEC variations is correlated with the height of tsunami, while longitudinal one is not. This is because, in the events that occurred along the coast, the height of tsunami is highly fluctuated due to the coast line. In such events, therefore, we determined the latitudinal width of TEC variations using ionospheric pierce points located on land-side. In the result, the correlation between the longitudinal distribution of TEC variations and the height of tsunami increased. Since the correlation between TEC variations and the height of tsunami is high, if events of the analysis target increase in the future, there is a possibility that the location, time and scale of the tsunami can be estimated.

Keywords: Total Electron Content, Earthquake

Improvement of high-latitude electric field model in GAIA

*Chihiro Tao¹, Hidekatsu Jin¹, Hiroyuki Shinagawa¹, Yasunobu Miyoshi², Hitoshi Fujiwara³, Mitsuru Matsumura⁴

1. National Institute of Information and Communications Technology, 2. Kyushu University, 3. Seikei University, 4. Institute for Space-Earth environmental Research, Nagoya University

GAIA (Ground-to-Topside Model of Atmosphere and Ionosphere for Aeronomy) solves physical and chemical dynamics of the whole atmosphere region from the troposphere to the exosphere under interactions with the ionosphere. Input from the polar region dramatically varies depending on the solar wind and magnetospheric conditions, which affects thermosphere and ionosphere globally. Total electron contents around Japan show discrepancy between observation and GAIA simulation without the polar input variation especially disturbed term. We are conducting improvement of the polar electric field input to GAIA referring to an empirical Weimer model which varies as a function of solar wind parameters. We will report the development and initial results in this presentation.

Keywords: thermosphere, ionosphere, simulation